JACS
JOURNAL OF THE AMERICAN CHEMICAL SOCIETY
Article
pubs.acs.org/JACS

Coordination Chemistry of Cyclic Disilylated Stannylenes and Plumbylenes to Group 4 Metallocenes

Henning Arp,[†] Judith Baumgartner,*[,†] Christoph Marschner,*[,†] Patrick Zark,[‡] and Thomas Müller*[,‡]

[†]Institut für Anorganische Chemie, Technische Universität Graz, Stremayrgasse 9, 8010 Graz, Austria

[‡]Institut für Reine und Angewandte Chemie, Carl von Ossietzky Universität Oldenburg, Carl-von-Ossietzky-Str. 9-11, 26111 Oldenburg, Federal Republic of Germany

Supporting Information

ABSTRACT: Reduction of group 4 metallocene dichlorides with magnesium in the presence of cyclic disilylated stannylene or plumbylene phosphine adducts yielded the respective metallocene tetrylene phosphine complexes. Under the same conditions the use of the respective dimerized stannylene or plumbylene gave metallocene ditetrylene complexes. A computational analysis of these reactions revealed for all investigated compounds multiple-bonded character for the M−E(II) linkage, which can be rationalized in the case of the monotetrylene complex with the classical σ-donor/π-acceptor interaction. The strength of the M−E(II) bond increases descending group 4 and decreases going from Sn to its heavier congener Pb. The weakness of the Ti−E(II) bonds is caused by the significantly reduced ability of the titanium atom for d−p π-back-bonding.

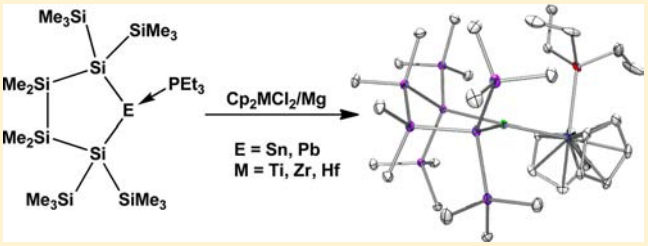

1. INTRODUCTION

The chemistry of heavier carbene analogues has attracted the attention of both experimentally and theoretically oriented chemists over the last decades.[1,2] The fundamental differences in electronic ground states, reactivities, and structures between carbenes and their heavier counterparts are certainly a major reason for this attraction. Heavy tetrylenes usually possess a singlet ground state with an increasing singlet−triplet gap with higher atomic number.[3] Responsible for this ground-state preference is a progressing reluctance to form hybrid orbitals. The s-electrons of the thus preferred $(ns)^2(np)^2$ configuration remain paired. As a consequence of this, dimerization of divalent species is not necessarily a favored process. Most heavier tetrylene dimers do not feature π-bonds, as common for olefins, but rather exist as dimeric donor−acceptor adducts. Attachment of electropositive substituents to the divalent group 14 atoms forces some mixing of their s- and p-orbitals. This way the singlet−triplet gap can significantly be diminished. Sekiguchi's distannene $(^t\mathrm{Bu}_2\mathrm{MeSi})_2\mathrm{Sn}{=}{=}\mathrm{Sn}(\mathrm{SiMe}^t\mathrm{Bu}_2)_2$, which, despite rather bulky groups on the tin atoms, does not dissociate into monomers in solution, is a good example for this behavior.[4] Descending group 14 further to lead, the reluctance to form dimeric compounds becomes even more pronounced. This is nicely illustrated by the difference between bis[tris(trimethylsilyl)silyl]tin and the analogous lead compound. While both compounds exist as monomers in solution, the stannylene crystallizes as a distannene, while the plumbylene retains its monomeric structure in the solid state.[5]

Recently, we could show that the bidentate tetrakis(trimethylsilyl)tetramethyltetrasilanylene ligand can be employed to stabilize divalent tin and lead compounds.[6,7] These can be isolated either as the respective base adducts (**1** and **2**) or as dimers (**3** and **4**). The dimeric stannylene and plumbylene compounds **3** and **4** exhibit considerable structural differences. While the tin compound **3** is the result of a dimerization−rearrangement process of a disilylated stannylene and exists as an endocyclic bicyclic distannene,[6] the plumbylene appears as a monomer in solution but crystallizes as a weak donor−acceptor adduct (**4**).[7]

In the present contribution we report on an extension of these studies to explore the coordination chemistry of disilylated stannylenes and plumbylenes with early transition metals and in particular with group 4 metallocenes. Only few examples of related compounds are known so far. In a seminal study Piers and co-workers[8,9] could demonstrate complexation of Lappert's stannylene[10] $\mathrm{Sn}[\mathrm{CH}(\mathrm{SiMe}_3)_2]_2$ to zirconocene derivatives. More recently reactions of C,N-chelated tin(II) and lead(II) compounds to zirconocene were reported by Ruzicka and co-workers.[11] In the latter case the employed plumbylene decomposed to elemental lead and free ligand during the reaction, thus no compound with a Zr−Pb bond was observed.[11] In this context also the formation of a hafnocene silylene complex, reported recently by Sekiguchi and co-workers, should be noted.[12] That the heavier tetrylenes can display quite different bonding motifs to transition metals has been shown recently by Hahn and co-workers.[13]

2. RESULTS AND DISCUSSION

Synthesis. For the synthesis of group 4 metallocene plumbylene and stannylene complexes a new general approach

Received: February 16, 2012
Published: June 20, 2012

   dx.doi.org/10.1021/ja301547x | J. Am. Chem. Soc. 2012, 134, 10864−10875

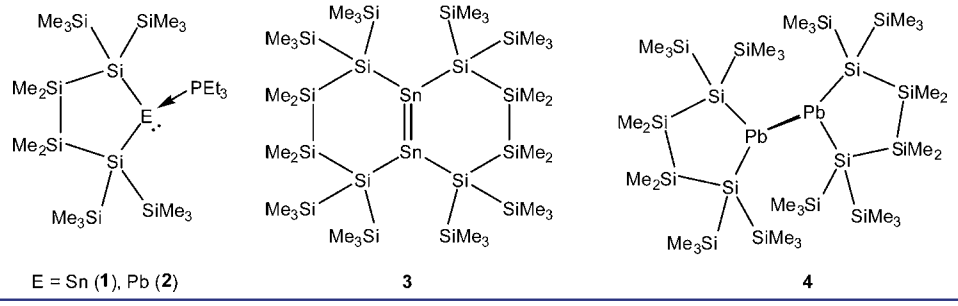

Scheme 1. Formation of Group 4 Metallocene Stannylene and Plumbylene Complexes

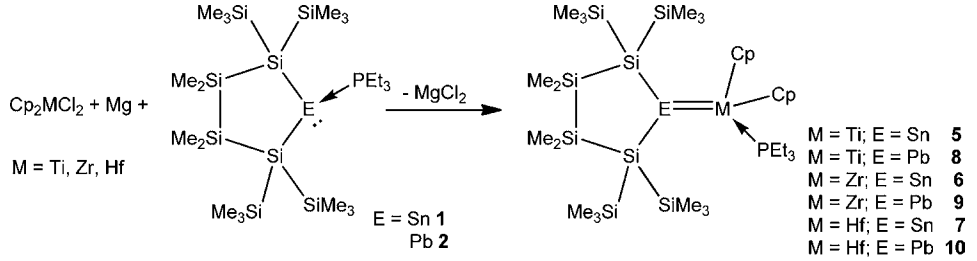

was sought. In the mentioned examples, the zirconocene stannylene complexes were prepared by warming Negishi zirconocene Cp_2ZrCl_2–2BuLi[14] in the presence of 2 equiv of stannylene from −80 °C to room temperature, thus limiting the scope of the reaction to zirconium.[8,9,11] Alternatively, we found that reductions of group 4 metallocene dichlorides with magnesium[15,16] in the presence of stannylene or plumbylene phosphine adducts (**1** and **2**) provided smooth conversion to the desired complexes (**5**–**10**) (Scheme 1). Isolated yields after crystallization from pentane of these highly colored compounds were above 80%. The plumbylene complexes of titanocene (**8**), zirconocene (**9**), and hafnocene (**10**) represent the first examples of compounds with group 4 metal–lead bonds. In general it should be noted that the number of known plumbylene transition-metal complexes is quite small.[17]

By reaction of 1,2-dipotassiodisilanes and -digermanes with metallocene dichlorides, we recently succeeded in the synthesis of group 4 disilene and digermene complexes.[18] When this reaction, however, was carried out with the respective 1,2-dipotassiodistannane, instead of the expected distannene complexes, metallacyclotetrastannanes were isolated as the only tin containing products.[18] This behavior of tin was attributed to its greater preference for the divalent state compared to its lighter congeneres.[18] As the distannene unit of **3** (Scheme 2) is held together by two bridging tetrasilanylene ligands, we reasoned that the dissociation to stannylenes might be blocked, and thus an equimolar amount of **3** could serve as a precursor for a distannene complex. However, when Cp_2HfCl_2 was reduced with magnesium in the presence of an equimolar amount of **3**, the only pentane soluble product was the hafnocene bis(stannylene) complex **11** (Scheme 2). Its formation is apparently facilitated by the reversible rearrangement of **3** to the exocyclic distannene isomer,[6] which is the direct dimerization product of the monomeric stannylene **12** (Table 2).[6] Coordination of the exocyclic distannene to the hafnocene would then favor the distannylene over the distannene complex as observed previously.[18]

Complex **11** was isolated in about 60% yield as thin almost black needles. Piers et al. briefly mentioned the possibility of replacing just one stannylene ligand in their zirconocene bis(stannylene) complex with PMe_3, but no detailed information on this reaction was provided.[9] Reaction of **11** with 2 equiv of PEt_3 in fact led to selective formation of **7** and **1** (Scheme 2). Reaction of **3** with Cp_2TiCl_2 and magnesium yielded the titanocene bis(stannylene) complex **13** (Scheme 2), but in this case, starting material **3** was contaminated with $KN(SiMe_3)_2$ leading in addition to the formation of the trivalent titanium compound $Cp_2TiN(SiMe_3)_2$ (**14**). The eventually obtained crystals contained **13** and **14** in a 1:1 ratio. An interesting aspect of these reactions is that attempts to react **3** with excess metallocene dichloride did not lead to monostannylene complexes but selectively to the distannylene compounds.

Under very similar conditions, employing magnesium reduction of hafnocene dichloride in the presence of 2 equiv of **4** even the hafnocene bis(plumbylene) complex **15** could be obtained in moderate yield (Scheme 3). Again, addition of PEt_3 to **15** led to the selective formation of plumbylene phosphine adduct **2** and hafnocene complex **10**. Due to the very high

Scheme 2. Formation of Hafnocene and Titanocene Bis(stannylene) Complexes 11 and 13

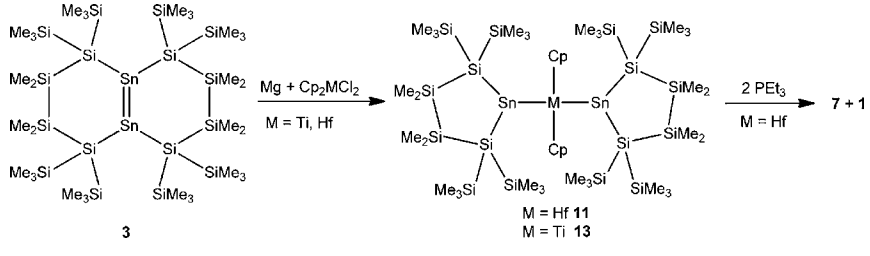

dx.doi.org/10.1021/ja301547x | J. Am. Chem. Soc. 2012, 134, 10864–10875

Scheme 3. Synthesis of Hafnocene Bis(plumbylene) Complex 15

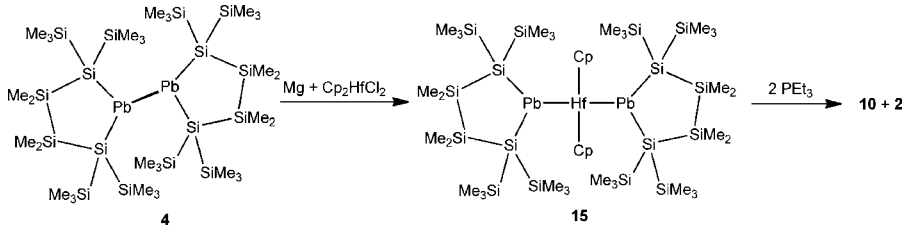

Scheme 4. Synthesis of zirconocene plumbylene THF complex 16

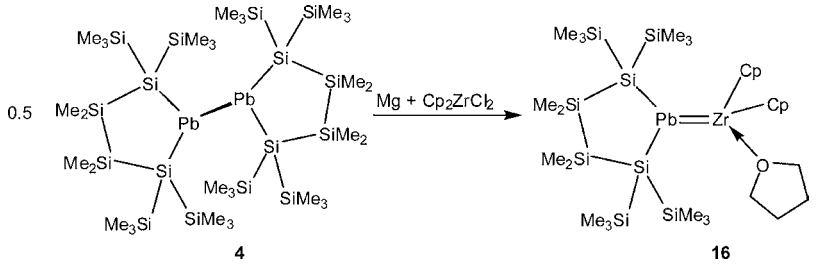

solubility in pentane of both **11** and **15**, they were difficult to isolate, and unfortunately only rather low-quality crystals could be obtained and used for X-ray diffraction experiments.

A reaction of Cp_2ZrCl_2 and magnesium with a substoichiometric amount of **4** (Scheme 4) was carried out to check whether the preference for the formation of ditetrylene complexes extends to lead. The formation of the zirconocene plumbylene complex **16**, where the vacant coordination site at zirconium is occupied by a THF molecule, showed this not to be the case.

In order to assess the general applicability of this simple access to group 4 metal tetrylenes, we reacted $TaCl_5$ as a group 5 compound with magnesium in the presence of stannylene adduct **1** (Scheme 5). The successful formation of a stannylene

Scheme 5. Synthesis of tantalum stannylene complex 17

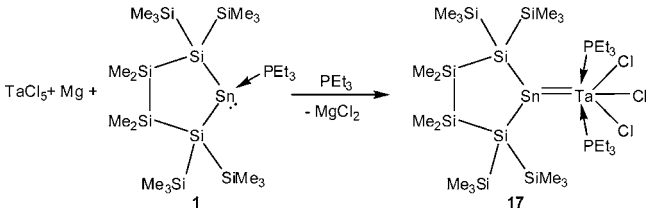

complex of $TaCl_3$, **17**, was confirmed by NMR spectroscopy, and a low-quality crystal structure, which revealed a distorted octahedral coordination geometry around tantalum with two trans-oriented PEt_3 ligands.

NMR Spectroscopy. Distannene **3** exhibits a typical distannene ^{119}Sn NMR shift of 545 ppm, strongly indicating the persistence of the Sn═Sn double bond in solution.[6] Further proof for the retained Sn−Sn bond in solution is the presence of ^{117}Sn satellites in the ^{119}Sn NMR spectrum of **3**. The coupling constant of $^1J_{(^{119}Sn/^{117}Sn)}$ = 1240 Hz is relatively small compared to a value of 2930 Hz found for Masamune's tetraaryldistannene,[19] suggesting only weak bonding of donor−acceptor type. By coordination of a phosphine ligand to the stannylene (**1**), electron octet configuration is achieved. Therefore, chemical shifts far upfield from those expected for the free stannylene **12** are observed. In **1** the ^{119}Sn resonance was found at −224 ppm,[6] consistent with the very recent report by Escudié and co-workers for the NHC adduct of bis[tris(trimethylsilyl)silyl]tin (δ = −197 ppm).[20] The ^{119}Sn NMR signal of **1** is split into a doublet by the adjacent ^{31}P nucleus with a coupling constant of 2220 Hz. The group 4 metallocene stannylene complexes **5**−**7** display downfield shifted ^{119}Sn resonances compared to **1**. The chemical shift of titanocene complex **5** was found to be 1635 ppm with the signal being a doublet with $^2J_{SnP}$ = 276 Hz coupling to phosphorus. The respective zirconocene and hafnocene complexes **6** and **7** exhibit their ^{119}Sn signals at considerably higher field at 1263 ppm (**6**, $^2J_{PSn}$ = 132 Hz) and 1080 ppm (**7**, $^2J_{PSn}$ = 92 Hz) with smaller coupling constants. The same trend can also be observed in the ^{31}P spectra of these complexes, as the chemical shift ranges from 50.2 ppm in the titanocene complex (**5**) down to 38.5 ppm for zirconium (**6**) to finally 34.8 ppm in the hafnium case (**7**) (Table 1). NMR spectroscopy thus clearly suggests an increasing degree of π-back-donation when descending group 4.

For the hafnium bis(stannylene) complex **11** the ^{119}Sn NMR resonance was found at a much lower field at 1785 ppm. This is in good agreement with the value of 1677 ppm observed by Piers and co-workers for their zirconocene bis(stannylene) complex.[9] The zirconocene bis(stannylene) complex published by Ruzicka and co-workers on the other hand resonates considerably upfield at 923 ppm.[11] However, the different behavior of the latter can be explained by intramolecular donation of electron density into the empty tin p-orbital from the attached amino groups of the parent stannylene. The difference between the ^{119}Sn NMR chemical shifts of **7** and **11** can be rationalized on the basis of π-back-donation. In **7** there is one phosphine and one stannylene ligand present, of which the first can be considered to be mainly a σ-donor. For this reason π-back-donation to tin is enhanced in this system, whereas in **11** the situation can be described as competition of two σ-donor π-acceptor ligands for the same electron pair. Therefore, the electronic environment approaches that of the free stannylene **12** and exhibits the pronounced downfield shift. While it is not completely clear how valid a comparison of the ^{119}Sn NMR shift of the tantalum compound **17** with the group 4 metallocene complexes of the same stannylene is, it seems fair to state that the chemical shift of δ = 1985 ppm is in the same

dx.doi.org/10.1021/ja301547x | J. Am. Chem. Soc. 2012, 134, 10864−10875

Table 1. Selected Spectroscopic and Structural Features of Group 4 Metallocene Tetrylene Complexes 5−10

compound	5	6	7	8	9	10
distance (Å) M−E	Ti−Sn 2.69	Zr−Sn 2.79	Hf−Sn 2.76	Ti−Pb 2.73	Zr−Pb 2.82	Hf−Pb 2.79
sum of covalent radii (Å)	2.99/2.76[a]	3.14/2.94[a]	3.14/2.92[a]	3.06/2.80[a]	3.21/2.98[a]	3.21/2.96[a]
range of known M−Sn single bond lengths (Å)[b]	2.81 − 2.89	2.93 - 3.09	2.91 - 3.06			
sum of angles around X (°)	359.6	359.5	359.6	359.6	359.6	359.7
	X = Sn	X = Sn	X = Sn	X = Pb	X = Pb	X = Pb
NMR (ppm)	^{119}Sn: 1635	^{119}Sn: 1263	^{119}Sn: 1080	^{207}Pb: 5299	^{207}Pb: 4165	^{207}Pb: 3462
	^{31}P: 50.2	^{31}P: 38.5	^{31}P: 34.8	^{31}P: 57.5	^{31}P: 46.3	^{31}P: 45.5
$^{2}J_{x}$ (Hz)	PSn: 276	PSn: 132	PSn: 92			

[a]Differences in the published values of tabulated covalent radii[22,23] of elements lead to different sums. [b]Obtained by searching for M−Sn single bond using CCDC's ConQuest 1.13.

region. The associated downfield shift compared to δ = 1080 ppm found for **7**, which contains also a third row transition metal and a phosphine ligand, is likely caused by a combination of several factors. Together with the fact that compound **17** is a 14 electron complex, the electronegative chloride substituents further diminish electron density at the metal. This certainly affects the ability of the tantalum atom to engage in back-donation.

Four signals in the ^{29}Si NMR spectrum of complex **11** indicate the equivalence of both five-membered rings in the complex. However, the two faces of each ring are not equivalent as two signals for the four $SiMe_3$ groups were observed. The same molecular symmetry was also derived from the respective ^{1}H and ^{13}C NMR spectra. This face differentiation suggests hindered rotation around the Zr−Sn bond in compound **11**.

The ^{207}Pb NMR spectroscopic results for the plumbylene complexes **8−10** show a similar trend as observed for their stannylene counterparts (**5−7**). A steady decrease in the chemical shift value descending group 4 was found: titanocene plumbylene complex **8** resonates at δ = 5299 ppm, zirconocene complex **9** at δ = 4165 ppm, and finally hafnocene plumbylene **10** at δ = 3462 ppm. The expected splitting into doublets caused by coupling to the ^{31}P nucleus of the phosphine ligand was not observed. The weaker bonds between Pb and the respective metal, compared to the analogous stannylene complexes, in addition to the fact that the ^{207}Pb signals are comparably broad [values for full width at half-maximum (fwhm) range from 130 to 220 Hz] seem to impede the observation of the $^{2}J_{PbP}$ coupling. ^{31}P NMR spectroscopic results for compounds **8−10** parallel the behavior observed for their lighter tin congeners. The ^{31}P NMR shifts are δ = 57.6, 46.3, and 45.5 ppm for **8−10**, respectively. The observed trend points again to a higher degree of back-bonding between the group 4 metal and Pb in Zr and Hf compounds **9** and **10** compared to titanocene complex **8**. The dependence of the M−E back-bonding from the additional phosphine ligands can be estimated from a comparison of the ^{207}Pb NMR chemical shifts of the plumbylene zirconocene **9** (δ = 4165 ppm) with the respective THF adduct **16** (δ = 5770). A downfield shift of ca. $\Delta\delta$ ^{207}Pb = 1600 ppm illustrates the superior electron-donating ability of the phosphine compared to THF.

Compared to a ^{207}Pb NMR chemical shift of δ = 3587 ppm reported for $[Fe(CO)_4]_4Pb$,[21] the strongly downfield shifted resonances between δ = 3462−5770 ppm for compounds **8−10** and **16** seem to indicate a marked plumbylene character. However, these chemical shifts have to be seen in the context of the free plumbylene, **18**, for which an extremely downfield shifted ^{207}Pb resonance at δ = 19516 ppm was found.[7] Compared to this, the plumbylene character of **8−10** and **16** seems to be not so pronounced.

The increasing electronic saturation of the Pb atom also can be observed in the ^{29}Si NMR spectra. In **8** the central silicon atoms resonate at δ = −16 ppm. With stronger π-back-bonding from the d^2 transition metal to the plumbylene, this resonance shifts upfield to δ = −42 and −54 ppm for **9** and **10**, respectively. Consistent with this argumentation, the comparison of **9** and **16** revealed a downfield shift of the ^{29}Si resonance of the silicon attached to Pb from δ = −42 ppm for **9** to δ = −37 ppm for **16**. The ^{29}Si signals for the more remote silicon atoms in **8−10** are found at almost identical positions, suggesting a very similar chemical environment. For **8−10** two different resonances for the trimethylsilyl groups were observed indicating hindered rotation around the metal−Pb bond and also no dissociation of phosphines. In contrast to this, only one $SiMe_3$ signal was observed for **16**, which suggests dissociation of THF, which can also be concluded from broadened signals in the respective ^{1}H spectrum. For hafnocene bis(plumbylene) complex **15** only ^{1}H, ^{13}C, and ^{29}Si NMR data could be obtained. The spectra for these nuclei are very similar to those of **11** and consistent with the proposed structure.

X-ray Crystallography. As all six phosphine tetrylene complexes (**5−10**) are isostructural, only one example of each group is shown [Figure 1: **7** and Figure 2: **10**; depictions of the others (**5**, **6**, **8**, and **9**) are available in the Supporting Information (Figures S1−S4)]. Compounds **5−10** feature planar geometries around the tetrel(II) center and short transition-metal tetrel(II) bond lengths. The sums of bond angles around tin or lead in all six examples match 360° almost exactly with a maximum deviation of 0.5°. The group 4−E (E = Sn or Pb) bond lengths are significantly shorter than the sum of tabulated covalent radii[22,23] or respective single bonds in the case of tin (Table 1). For lead this comparison cannot be made, as compounds containing Ti, Zr, or Hf bonds to Pb have not been reported so far. The X-ray crystallographic study strongly supports the conclusions drawn from the NMR observations with respect to the extent of bond order between the group 4 transition metals and tin or lead. Interesting in this respect is also the P transition-metal−E (E = Sn or Pb) angle of 90° in all compounds that ensures non-disturbance of the transition-metal interaction by the orthogonally coordinated phosphine ligand.

The crystals obtained of hafnocene bis(stannylene) **11** and hafnocene bis(plumbylene) **15** were not of high enough quality to permit a detailed structural discussion, therefore no metrical data can be given. But these structures (Figures S5 and S6, Supporting Information) still serve as proof for the atom connectivity and therefore validate the assignments made based

dx.doi.org/10.1021/ja301547x | J. Am. Chem. Soc. 2012, 134, 10864−10875

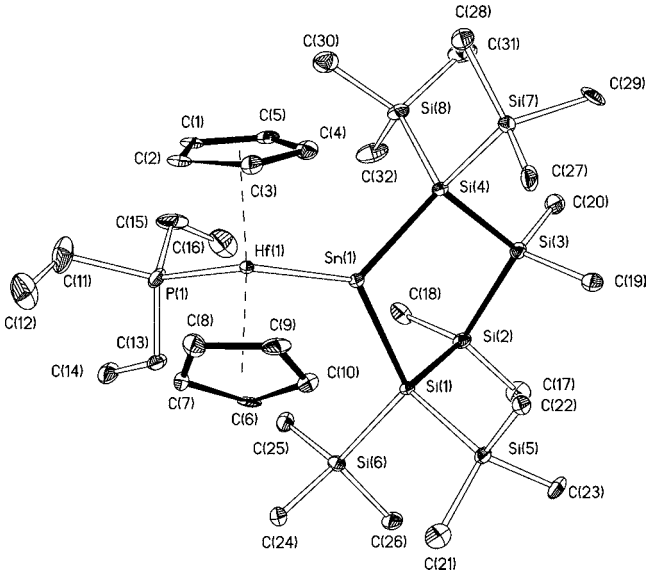

Figure 1. Molecular structure of **7** (thermal ellipsoid plot drawn at the 30% probability level). Hydrogen atoms omitted for clarity (bond lengths in Å, angles in °). Hf(1)−P(1) 2.663(3), Hf(1)−Sn(1) 2.7585(11), P(1)−C(13) 1.826(9), Si(1)−Si(2) 2.356(4), Si(1)−Sn(1) 2.626(2), Si(2)−C(17) 1.889(10), Si(4)−Sn(1) 2.622(3), P(1)−Hf(1)−Sn(1) 90.53(7), Si(4)−Sn(1)−Si(1) 99.41(8), Si(4)−Sn(1)−Hf(1) 129.95(6), Si(1)−Sn(1)−Hf(1) 130.25(6).

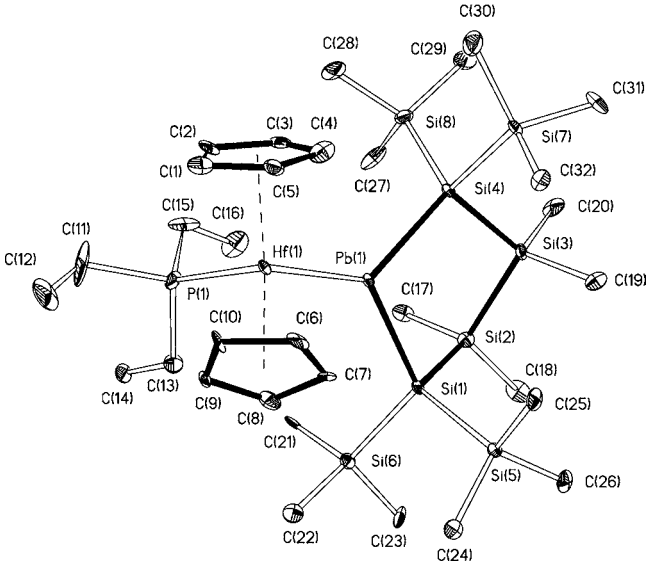

Figure 2. Molecular structure of **10** (thermal ellipsoid plot drawn at the 30% probability level). Hydrogen atoms omitted for clarity (bond lengths in Å, angles in °). Hf(1)−P(1) 2.670(5), Hf(1)−Pb(1) 2.7927(12), P(1)−C(11) 1.830(19), Pb(1)−Si(4) 2.690(5), Pb(1)−Si(1) 2.705(4), Si(1)−Si(2) 2.362(7), Si(2)−C(17) 1.889(17), C(15)−C(16) 1.55(3), P(1)−Hf(1)−Pb(1) 90.13(12), Si(4)−Pb(1)−Si(1) 98.24(14), Si(4)−Pb(1)−Hf(1) 130.62(10), Si(1)−Pb(1)−Hf(1) 130.81(10).

on NMR spectroscopy. The crystals containing titanocene bis(stannylene) **13** (Figure 3) together with $Cp_2TiN(SiMe_3)_2$ (**14**, Figure 4) in a 1:1 ratio were of much better quality. The bond lengths of Ti−Sn in **13**, with 2.71 and 2.72 Å, reflect the diminished degree of back-bonding compared to **5** (2.69 Å). The structure of compound **14** is also interesting as it

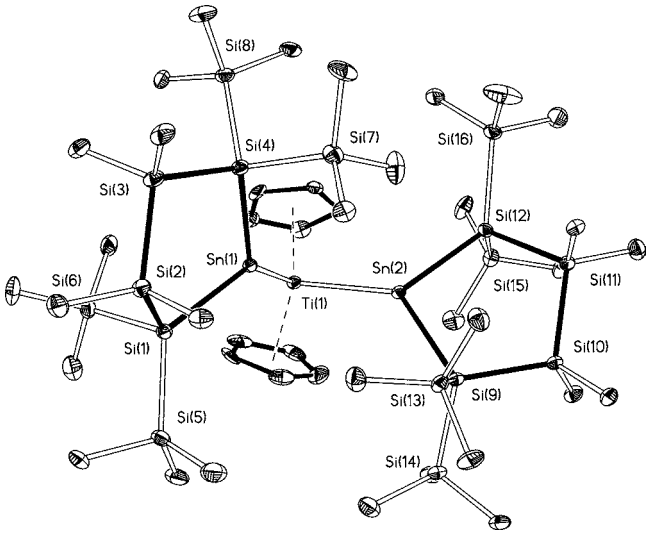

Figure 3. Molecular structure of **13** (thermal ellipsoid plot drawn at the 30% probability level). Hydrogen atoms omitted for clarity (bond lengths in Å, angles in °). Ti(1)−Sn(1) 2.7122(13), Ti(1)−Sn(2) 2.7154(14), Sn(1)−Si(4) 2.6399(19), Sn(1)−Si(1) 2.6570(19), Sn(2)−Si(9) 2.639(2), Sn(2)−Si(12) 2.6577(19), Sn(1)−Ti(1)−Sn(2) 88.98(4), Si(4)−Sn(1)−Ti(1) 132.35(5), Si(1)−Sn(1)−Ti(1) 126.06(5), Si(9)−Sn(2)−Si(12) 98.36(6), Si(9)−Sn(2)−Ti(1) 132.67(5), Si(12)−Sn(2)−Ti(1) 126.22(5).

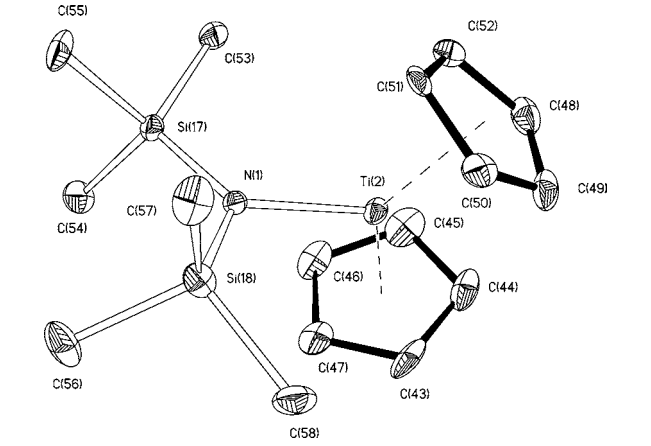

Figure 4. Molecular structure of **14** (thermal ellipsoid plot drawn at the 30% probability level). Hydrogen atoms omitted for clarity (bond lengths in Å, angles in °). Ti(2)−N(1) 2.020(6), N(1)−Si(18) 1.710(6), N(1)−Si(17) 1.722(6), Si(18)−N(1)−Si(17) 122.4(3), Si(18)−N(1)−Ti(2) 117.8(3), Si(17)−N(1)−Ti(2) 119.8(3).

represents a rare example of a structurally characterized titanocene amide with Ti in the oxidation state +3.[24,25]

Theoretical Studies.[26] Optimizations of the molecular structures of the free tetrylenes **12** and **18**, the group 4 element mono(tetrylene) complexes **5**−**10**, and the metallocenes bis(tetrylene) complexes **11**, **13**, **15**, and **19**−**21** at the density functional M06-2X/SDD (Sn, Pb, Ti, Zr, Hf) and 6-31G(d) (P, Si, C, H) level of theory result in structural parameters which are very close to those found by X-ray diffraction methods for some of these compounds. Data which are important for the discussion are summarized in Table 2. For the tetrylenes **12** and **18** for which no experimental structural data are available, half-chair conformations of the metallacyclopentasilane rings were predicted with the heavy group 14 element and the two neighboring silicon atoms spanning the

dx.doi.org/10.1021/ja301547x | J. Am. Chem. Soc. 2012, 134, 10864−10875

Table 2. Selected Experimental and Calculated [in parentheses, at M06-2X/SDD (M,E), 6-31G(d) (Si,C,H)] Structural Parameter, WBI, Molecular Orbital Energy Differences Δ*E* and Experimental Element NMR Chemical Shifts for Tetrylenes 12, 18, Monotetrylene Complexes 5−10, and Bis-tetrylene Complexes of Group 4 Metallocenes 11, 13, 15, 19−21[a]

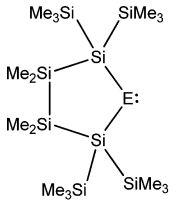

E	
Sn	**12**
Pb	**18**

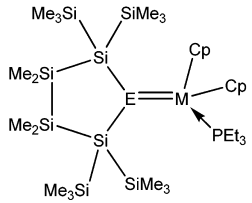

E/M	Ti	Zr	Hf
Sn	**5**	**6**	**7**
Pb	**8**	**9**	**10**

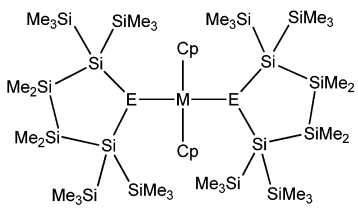

E/M	Ti	Zr	Hf
Sn	**13**	**19**	**11**
Pb	**20**	**21**	**15**

compd	M−E	*d*(M−E) [pm]	*d*(E−Si) [pm]	α(E,M,P) [°]	α(Si,E,Si) [°]	WBI (ME)	$\Delta E(d_{xz}/\pi)^b$ [eV]	$\Delta E(p_x/\pi^*)^b$ [eV]	$\Delta E^{para\ b}$ [eV]	δ^{ISO}E expt	BDE (ME) [kJ mol^{-1}]	BDE^{B3LYP} (ME) [kJ mol^{-1}]	BDE^{NCI} (ME) [kJ mol^{-1}]
5	Ti−Sn	269.4(265.3)	264.7(267.5)	89.5 (91.1)	99.1 (98.3)	1.23	0.27	1.21	5.20	1635[c]	151	70	81
6	Zr−Sn	279.4(278.0)	263.6(265.9)	90.8 (92.0)	99.3 (98.8)	1.52	0.60	1.42	5.45	1263[c]	249	162	87
7	Hf−Sn	275.9(278.3)	262.4(265.2)	90.5 (92.0)	99.4 (99.1)	1.58	0.66	1.55	5.57	1080[c]	270	180	90
8	Ti−Pb	272.7(275.4)	271.1(274.1)	89.2 (90.6)	97.8 (95.9)	1.07	0.34	0.96	5.04	5299[d]	118	58	60
9	Zr−Pb	282.1(284.3)	270.8(272.4)	90.1 (92.2)	98.0 (97.5)	1.38	0.62	1.25	5.40	4165[d]	215	145	70
10	Hf−Pb	279.3(284.2)	269.7(271.7)	90.1 (92.2)	98.2 (97.2)	1.44	0.67	1.40	5.83	3462[d]	234	161	73
12	Sn		(267.4)		(91.7)								
18	Pb		(275.1)		(90.5)					19516[d]			
13	Ti−Sn	271.4(269.3)	264.8(267.1)	89.0 (86.1)	98.4 (97.6)	1.07				2172[c]	153[e]	60[e]	93
19	Zr−Sn	(285.3)	(267.3)	(90.1)	(97.6)	1.19					222[e]	133[e]	89
11	Hf−Sn	(286.1)	(267.1)	(90.2)	(97.7)	1.22				1785[c]	239[e]	151[e]	88
20	Ti−Pb	(280.0)	(274.6)	(87.5)	(95.9)	0.93					120[e]	47[e]	73
21	Zr−Pb	(291.6)	(273.8)	(89.1)	(96.5)	1.15					193[e]	116[e]	77
15	Hf−Pb	(291.6)	(273.5)	(88.7)	(96.6)	1.15					209[e]	132[e]	77

[a]BDE of the ME bonds calculated using the M06-2X functional are given as BDE(ME). For comparison, the BDE computed applying the B3LYP functional, here denoted as BDE^{B3LYP}(ME), is summarized as well. Finally, the noncovalent contributions to the BDE, BDE^{NCI}(ME), calculated from the difference between BDE(ME) and BDE^{B3LYP}(ME) are listed. [b]For definition see Figure 5. [c]^{119}Sn NMR [d]^{207}Pb NMR. [e]Mean value computed from the dissociation of the complex into a Cp_2M fragment and two tetrylenes.

dx.doi.org/10.1021/ja301547x | J. Am. Chem. Soc. 2012, 134, 10864−10875

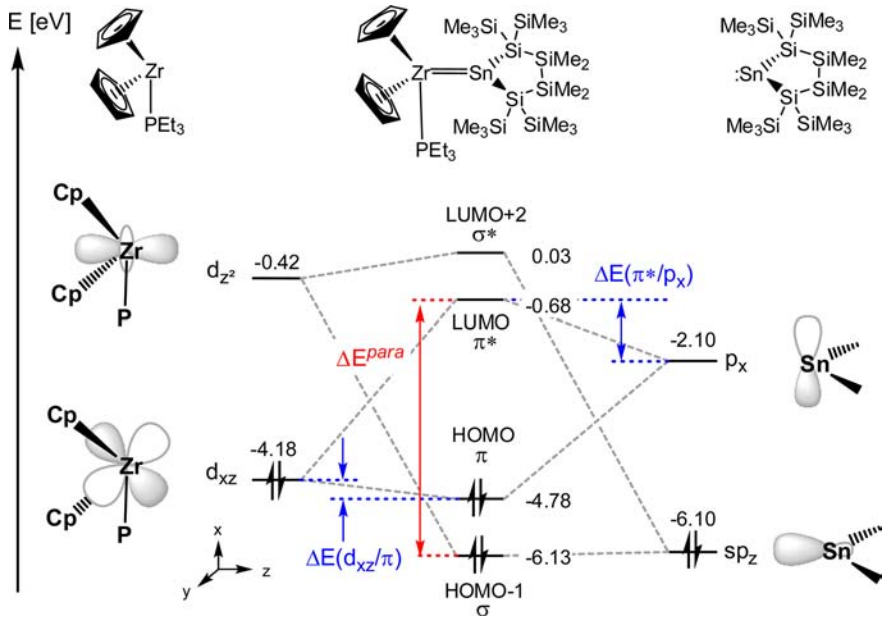

Figure 5. FMO interaction scheme for monotetrylene complex **6,** derived from M06-2X/SDD (Zr, Sn), 6-31G(d) (Si, P, C, H) calculations. This MO scheme is qualitatively valid for all investigated monotetrylene complexes **5**−**10**.

central plane.[27] A common feature of all optimized molecular structures of the mono(tetrylene) (**5**−**10**) and of the metallocene bis(tetrylene) complexes **11**, **13**, **15**, and **19**−**21** are trigonal planar coordinated Sn or Pb atoms (sum of the bond angles α around the element atom, $\Sigma\alpha$(E) = 358−360°) embedded in a half-chair metallacyclopentasilane ring of local C_2 symmetry. The computational results indicate no significant influence of the complexation on the molecular structure of the tetrylene. The most obvious structural modification is a widening of the endocyclic SiESi bond angle α(SiESi) by 5.4−7.4° (see Table 2). In accordance with the available experimental structures, the results of the computation predict that the tetrylene units are oriented mostly perpendicular to the central E−M−P plane in tetrylene complexes **5**−**10** (dihedral angle β = 82−84°),[28] while in the metallocene bis(tetrylene) complexes **11**, **13**, **15**, and **19**−**21**, the equivalent dihedral angle is somewhat smaller (β = 65−74°).[28] This specific arrangement allows for an efficient back-bonding from metal d-orbitals to the formally empty p-orbital at the tetrel atom. The calculated M−E(II) bond lengths, which are summarized in Table 2, show the expected trends. That is, for a given tetrylene the E−M distances increase along the series E−Ti < E−Zr ∼ E−Hf, and the Sn−M separations are always smaller than the corresponding Pb−M distances. The calculated M−E(II) bond lengths as well as those determined experimentally (see Table 2) are all smaller than standard values for E−M single bonds (Sn−M: 276 pm (Ti), 294 pm (Zr), 292 pm (Hf); Pb−M: 280 pm (Ti), 298 pm (Zr), 296 pm (Hf)),[23] in no case, however, the values predicted for $\sigma^2\pi^2$ E═M double bonds are reached (Sn═M: 247 pm (Ti), 257 pm (Zr), 258 pm (Hf); Pb═M: 252 pm (Ti), 262 pm (Zr), 263 pm (Hf)).[23] In agreement with these structural criteria also, the results of a natural bond orbital (NBO) analysis indicate the multiple-bond character for the M−E(II) linkage in mono- and bis(tetrylene) complexes **5**−**10**, **11**, **13**, **15**, **19**−**21** (see Table 2). In detail, all calculated Wiberg bond indices (WBIs) are significantly larger than computed for the respective M−E(IV) single bond in the corresponding metallocene−ditetryl compound ($Cp_2M(EMe_3)_2$)[E = Sn: 0.83 (Ti), 0.93 (Zr), 0.94 (Hf); E = Pb: 0.79 (Ti), 0.91 (Zr), 0.92 (Hf)]. As it is expected, the WBIs for the M−E(II) bond for stannylene complexes are always larger than computed for the corresponding plumbylene complex, and the calculated bond orders for the M−E(II) bond, as expressed by the WBIs, increase for a given tetrel element in the order Ti < Zr ≤ Hf. In addition the calculated bond order is for each M−E pair larger for the mono(tetrylene) complex than for the metallocene bis(tetrylene). These trends are also reflected by the computed bond dissociation energies for the M−E(II) bond BDE(ME) for the tetrylene complexes (see Table 2). The E−Ti bonds are significantly less stable than the E−Zr bonds [by 97 (**5**/**6**) and 98 kJ mol^{-1} (**8**/**9**) in the case of the mono(tetrylene) complexes and by 68 (**13**/**19**) and 72 kJ mol^{-1} (**20**/**21**) for the bis(tetrylene) complexes], and there is a second although smaller increase predicted for the BDE of the E−Hf bonds (by 17−21 kJ mol^{-1}). The Pb−M bonds are for all calculated metallocene complexes 29−36 kJ mol^{-1} weaker than the corresponding Sn−M linkages. The BDE values for the Ti−E bonds in mono(tetrylene) (**5**, **8**) and bis(tetrylene) complexes **13**, **20** are very similar (see Table 2). The situation differs, however, for the hafnocene and zirconocene complexes for which the computed BDEs of the M−E(II) bond are smaller in bis(tetrylene) complexes than in their mono(tetrylene) counterparts by 18−31 kJ mol^{-1}.

The bonding between the zirconium and the tin atoms in the mono(tetrylene) complex **6** is rationalized by the orbital interaction diagram shown in Figure 5. This orbital interaction diagram is also valid qualitatively for all investigated metallocene mono(tetrylene) complexes **5**−**10**. Plots of the surface diagrams for frontier molecular orbitals (FMOs) of compound **6** can be found in the Supporting Information. The M−E(II) bond in complexes **5**−**10** is best described by the conventional σ-bonding/(d/p) π-back-bonding scheme for carbene complexes. In the framework of perturbation theory, the relative extent of back-bonding in the metallocene tetrylene complexes can be estimated by the evaluation of the calculated orbital stabilization energy $\Delta E(d_{xz}/\pi)$ and the corresponding destabilization

dx.doi.org/10.1021/ja301547x | J. Am. Chem. Soc. 2012, 134, 10864−10875

energy $\Delta E(\pi^*/p_x)$ (see Figure 5 and Table 2). Both energy differences increase for both kinds of metallocene mono-(tetrylene) complexes along the series Ti < Zr < Hf. This suggests that the $d_{xz} \rightarrow p_x$ π-back-bonding is smallest for the titanium complexes (**5**, **8**) and largest for the hafnium compounds (**7**, **10**).

The analysis also indicates that for each group 4 metallocene, the lowering of the π-orbital as expressed by $\Delta E(d_{xz}/\pi)$ is slightly smaller in the stannylene complexes (**5**−**7**) than in the corresponding plumbylene complexes (**8**−**10**, by 0.07 eV (Ti), 0.02 eV (Zr), 0.01 eV (Hf)). On the other hand, the effect of the tetrylene on the π^* level is more significant, as the destabilization energy $\Delta E(\pi^*/p_x)$ is markedly larger for the stannylene complexes (**5**−**7**) than for the corresponding plumbylene complexes (**8**−**10**, by 0.25 eV (Ti), 0.17 eV (Zr), 0.15 eV (Hf)).

The poor ability of the titanocene to engage in π-bonding is mostly due to the poor spatial and energetic match between the $3d_{xz}$ orbital of titanium and the $5p_x$ orbital of the tin ($\Delta E(d_{xz}/p_x)$ = 2.65 vs 2.08 eV for Zr or 1.88 eV for Hf) or $6p_x$ of lead atom (($\Delta E(d_{xz}/p_x)$ = 2.80 vs 2.22 eV for Zr or 2.03 eV for Hf).

NMR chemical shifts of group 14 carbene analogs are always extremely large due to a dominant paramagnetic contribution, which arises from the efficient interaction of the applied magnetic field with the filled sp_z-type MO and the orthogonal empty p-type orbital at the dicoordinated tetrel element.[29] The paramagnetic shift is very large for small energy differences ΔE^{para} between these two magnetically active orbitals.[29] In the mono(tetrylene) complexes the sp_z orbital is transformed to the σ-orbital of the M−E(II) bond, and the p_x orbital can be associated with the π^*-orbital (Figure 5). Therefore, the ^{119}Sn NMR chemical shift of the stannylene complexes **5**−**7** and the ^{207}Pb NMR chemical shift of the metallocene plumbylene complexes **8**−**10** are determined mainly by the energy difference between these two molecular orbitals, ΔE^{para} (see Figure 5). While the energy of the σ-orbital remains nearly constant for a given tetrel element along the series of group 4 metals ($E(\sigma)$ = −6.09 eV (**5**), −6.13 eV (**6**), −6.12 eV (**7**)), the π^*-level is significantly altered by the different extent of back-bonding ($E(\pi^*)$ = −0.90 eV (**5**), −0.68 eV (**6**), −0.55 eV (**7**)).[30] Consequently, the changes in ΔE^{para}, summarized in Table 2, are mostly due to the different extent of back-bonding in that sense as the larger ΔE^{para}, the higher the multiple-bond character of the M−E(II) bond. Therefore the experimental ^{119}Sn NMR chemical shift of stannylene compounds **5**−**7** and the experimental ^{207}Pb NMR shift of the metallocene plumbylene complexes **8**−**10** can be used as a tool to estimate the degree of multiple bonding in these complexes. Increasing multiple-bond character of the M−E(II) bond leads to increasing energy differences ΔE^{para}, which becomes manifest in a upfield shift of the element resonance in NMR spectroscopy. These relations become obvious by analyzing the data summarized in Table 2, and although only a very limited set of data is used, by the correlations between the reciprocal calculated ΔE^{para} and the experimental chemical shifts δ^{119}Sn (**5**−**7**) and δ^{207}Pb (**8**−**10**) shown in Figure 6.

The bonding in bis(stannylene) zirconocenes was treated principally already by Piers.[9] In agreement with that earlier investigation we found that multicenter interactions are important for the understanding of the bonding in bis-(tetrylene) complexes **11**, **13**, **15**, and **19**−**21**. The FMO interaction diagram of the bis(stannylene) zirconocene **19** is shown in Figure 7. Qualitatively, it is also valid for the

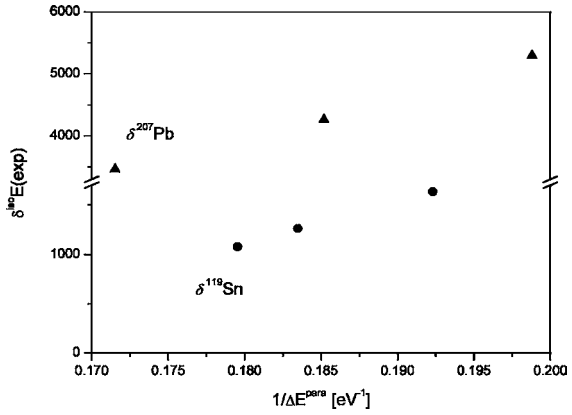

Figure 6. Plot of the experimental δ ^{119}Sn (●) and δ ^{207}Pb NMR (▲) chemical shifts versus the reciprocal ΔE^{para} for monostannylene complexes **5**−**7** and monoplumbylene metallocenes **8**−**10**.

investigated bis(tetrylene) complexes **11**, **13**, **15**, **20**, and **21**. The analysis reveals that the $ME(II)_2$ group is built up by two σ-type orbitals and the π-type HOMO, each delocalized across all three constituent atoms (see Figures 7 and 8 for surface diagrams of the respective MOs). The delocalization of the π-type HOMO across all three atoms helps to rationalize the smaller bond order and the weaker M−E(II) bond in group 4 metallocene bis(tetrylene) complexes compared to their mono(tetrylene) counterparts. In addition, inspection of the HOMO of compound **19** indicates some degree of bonding interaction between the two distant Sn atoms, although their separation, d(SnSn), approaches the sum of the van der Waals radii, ΣvdWR (d(SnSn) 403.8 pm, ΣvdWR 434 pm).[31] The computed WBI index between this pair of atoms differs significantly from zero; it is however only 22% of the bond index computed at the same theoretical level for the central Sn−Sn single bond in $(H_3Si)_6Sn_2$ (**19**: WBI(SnSn) = 0.20; $(H_3Si)_6Sn_2$: WBI(SnSn) = 0.92, d(SnSn) = 283.7 pm). Similar small WBIs were computed for the bis-(tetrylene) complexes **11**, **13**, **15**, **20**, and **21** (WBIs range from 0.15 (PbPb in complex **20**) to 0.23 (SnSn in compound **11**)). These computational data suggest that in the continuum of possible bonding modes for group 4 metallocene bis(tetrylene) complexes, beginning with the ditetren complex **A**, passing the metallacyclopropane **B** and ending at the delocalized bis(tetrylene) structure **C**, the here investigated complexes **11**, **13**, **15** and , **19**−**21** are best described by canonical structure **C** with only minor contribution from structure **B** (Scheme 6).

The large and polarizable substituents which are present in all investigated metallocene complexes suggest that attractive dispersion energy contributions to the overall binding energy of the complexes might be a decisive factor. The here applied M06-2X functional[32] properly accounts for dispersion forces, while the most prominent deficit of the popular B3LYP functional is the nearly complete negligence of noncovalent van der Waals interactions. Therefore, the difference in the calculated bond dissociation energies (BDEs) using these two functionals allows estimating the contribution of noncovalent bonding in metallocene complexes **5**−**11**, **13**, **15**, and **19**−**21**.[33−35] The contribution of noncovalent interactions, BDE^{NCI}, to the overall BDE, which is calculated as the difference between the BDE obtained at the M06-2X level and the reduced BDE^{B3LYP} obtained at the B3LYP level (see Table 2), is

dx.doi.org/10.1021/ja301547x | J. Am. Chem. Soc. 2012, 134, 10864−10875

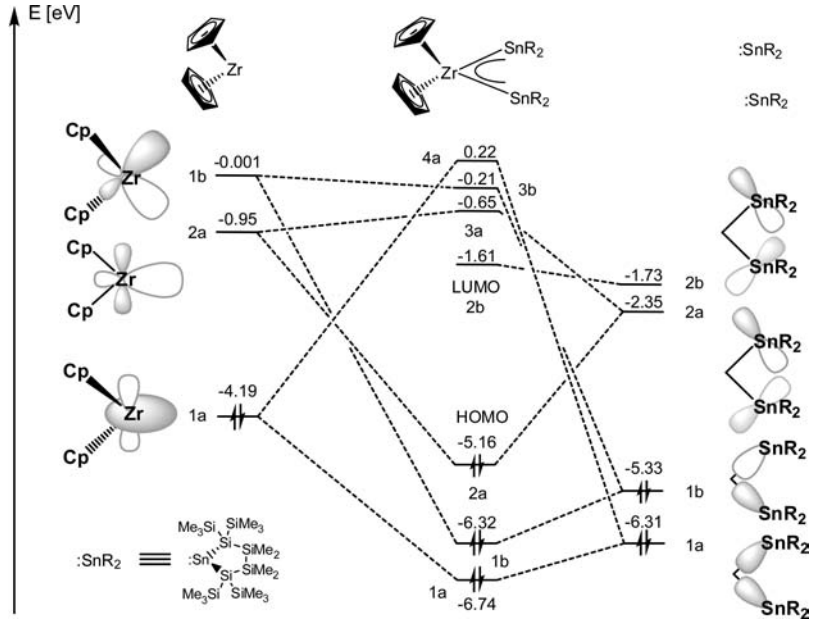

Figure 7. FMO interaction scheme for bis(tetrylene) complex **19** in C_2 symmetry, derived from M06-2X/SDD(Zr,Sn), 6-31G(d) (Si,C,H) calculations. The FMO diagram for Cp_2Zr is derived from that of $Cp_2Zr(PEt_3)$ (see Figure 5) by removal of the phosphane ligand (see the Supporting Information for further details). This MO scheme is qualitatively valid for all investigated bis-tetrylene complexes **11**, **13**, **15**, and **19**–**21**.

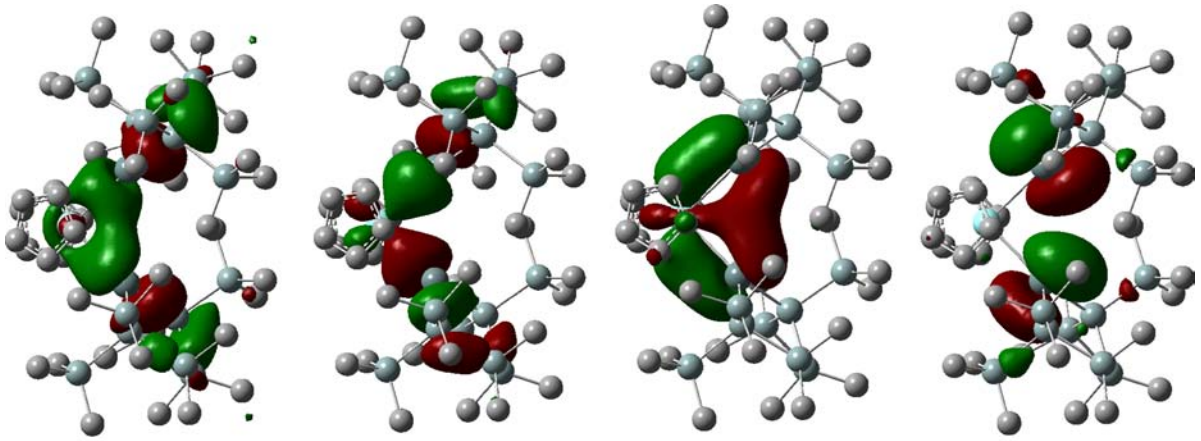

Figure 8. Calculated surface diagrams for pertinent molecular orbitals of bis(stannylene) complex **19** in C_2 symmetry, derived from M06-2X/SDD(Zr,Sn), 6-31G(d) (Si,C,H) calculations (isodensity value: 0.05). (a) 1a orbital (σ-EME bonding (HOMO-4)); (b) 1b orbital (σ EME bonding (HOMO-1)); (c) 2a orbital (π EME bonding (HOMO)); (d) 2b orbital (π EME nonbonding (LUMO)) (Color code: light blue: Zr, greenish gray: Sn; blue gray: Si; and gray: carbon).

Scheme 6. Possible Structural Arrangements Group 4 Metallocene Bis(tetrylene) Complexes (M = Ti–Hf; E = Sn, Pb).

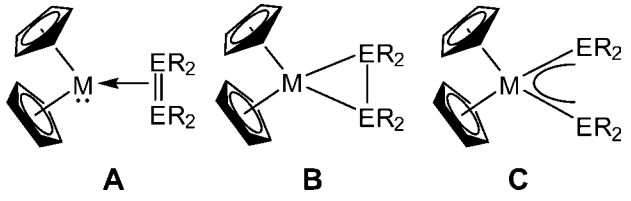

substantial in all cases. In the case of the titanium complexes it accounts for 60% of the overall BDE and even in the hafnium complexes it amounts to 30%.

3. CONCLUSION

The present study demonstrates that stannylene and plumbylene complexes of all three group 4 metallocenes are synthetically accessible by magnesium reduction of the corresponding metallocene dichlorides in the presence of the phosphine-stabilized tetrylenes **1** or **2**. Significant π back-bonding from the transition metal to the heavy main group atom was shown by NMR spectroscopy and confirmed by X-ray structure analyses of all six complexes **5**–**10**. The stannylene complexes **5** and **7** are the first stannylene complexes of titanium and hafnium to be reported, whereas **8**–**10** are the first compounds to feature group 4–lead bonds at all. Using the base-free compounds **3** and **4** hafnocene bis(tetrylene) complexes, **11** and **15**, could be prepared. In these complexes the extent of π-back-bonding is

decreased because of competition of two π-acceptor ligands for only one electron pair.

The theoretical analysis of the bonding in metallocene mono- and bis(tetrylene) complexes **5**−**10**, **11**, **13**, **15**, and **19**−**21** revealed for all investigated compounds multiple-bonded character for the M−E(II) linkage in agreement with the interpretation of the experimental data. The bonding between the group 4 metal and the group 14 element atom can be rationalized in the case of the mono(tetrylene) complexes with the classical σ-donor−π-acceptor interaction. The strength of the M−E(II) linkage increases descending the group 4 metals and decreases going from Sn to its heavier congener Pb. As a consequence, the weakest M−E(II) bonds are found between Ti and Pb atoms, while the strongest are predicted by the computation for the pair Hf−Sn. The reason for the weakness of the Ti−E(II) bonds is the significantly reduced ability of the titanium atom for d−p π-back-bonding. The theoretical analysis of the bonding in mono(tetrylene) complexes **5**−**10** supports the presumption based on experimental data that the NMR chemical shift of the tetrel atom in the complex is a qualitative measure for the extent of multiple-bonding between the metal and the tetrel atom in these complexes. Increased d−p back-bonding results in significant shielding of the tetrel atom. The calculated WBIs and BDEs indicate that the individual M−E(II) bond is weaker in the bis(tetrylene) zirconocene and hafnocene complexes **11**, **15**, **19**, and **21** than in the corresponding mono(tetrylene) complexes **6**, **7**, **9**, and **10**. Clearly, this is a result of the reduced multiple-bond character of the M−E(II) linkage, due to the competition between two acceptor π-type orbitals for one metal d-orbital in the metallocene bis(tetrylene) complexes. This situation is best described by a multicenter bonding which involves the two tetrel atoms and the central metal atom. The degree of Ti−E π-back-bonding in the titanium complexes **5** and **8** is already small and is not further reduced by the addition of a second tetrylene unit in complexes **13** and **20**. Consequently, similar BDEs for the Ti−E(II) bonds in compounds **5**, **8**, **13**, and **20** are predicted by the calculations.

4. EXPERIMENTAL SECTION

General Remarks. All reactions involving air-sensitive compounds were carried out under an atmosphere of dry nitrogen or argon using either Schlenk techniques or a glovebox. All solvents were dried using column-based solvent purification system.[36] Chemicals were obtained from different suppliers and used without further purification.

^{1}H (300 MHz), ^{13}C (75.4 MHz), ^{29}Si (59.3 MHz), ^{31}P (124.4 MHz), ^{119}Sn (111.8 MHz), and ^{207}Pb (62.8 MHz) NMR spectra were recorded on a Varian INOVA 300 spectrometer. If not noted otherwise for all samples, C_6D_6 was used as solvent. To compensate for the low isotopic abundance of ^{29}Si, the INEPT pulse sequence[37,38] was used for the amplification of the signal. Elemental analyses were carried out using a Heraeus VARIO ELEMENTAR instrument. For the plumbylene complexes, attempts to obtain elemental analysis data gave consistently too low values for C and H.

X-ray Structure Determination. For X-ray structure analyses the crystals were mounted onto the tip of glass fibers, and data collection was performed with a BRUKER-AXS SMART APEX CCD diffractometer using graphite-monochromated Mo Kα radiation (0.71073 Å). The data were reduced to F_o^2 and corrected for absorption effects with SAINT[39] and SADABS,[40,41] respectively. The structures were solved by direct methods and refined by full-matrix least-squares method (SHELXL97).[42] If not noted otherwise, all non-hydrogen atoms were refined with anisotropic displacement parameter. All hydrogen atoms were located in calculated positions to correspond to standard bond lengths and angles. All diagrams were drawn with 30% probability thermal ellipsoids, and all hydrogen atoms were omitted for clarity. Unfortunately the obtained crystal quality of some substances was poor. This fact is reflected by quite high R and low θ values.

Crystallographic data (excluding structure factors) for the structures of compounds **5**−**11** and **13**−**15** reported in this paper have been deposited with the Cambridge Crystallographic Data Center as supplementary publication no. CCDC-831742 (**5**), 831743 (**6**), 831744 (**7**), 831751 (**8**), 831748 (**9**), 831745 (**10**), 855936 (**11**), 855938 (**13** and **14**), and 855937 (**15**). Copies of data can be obtained free of charge at: http://www.ccdc.cam.ac.uk/products/csd/request/.

Compounds **1**,[6] **2**,[7] **3**,[6] and **4**[7] were prepared according to published procedures.

General Procedure. For group 4 metallocene monotetrylene complexes **5**−**10**: An equimolar (0.5 mmol each) mixture of group 4 metallocene dichloride, magnesium turnings, and **1** or **2** was stirred in THF (5 mL) for 3 h. During this time deeply colored solutions formed. The THF was removed under reduced pressure, and the remaining solid was extracted with pentane (3×, 5 mL each). The filtrate was concentrated to 6 mL and stored at −60 °C for 16 h. Crystals could be isolated by decantation. Typical yield: about 80%.

*Titanocene Stannylene Phosphine Complex (**5**).* Dark-blue crystals (yield: 81%): ^{1}H NMR (δ in ppm): 5.24 (s, 10H, Cp), 1.05 (m, 9H, $P(CH_2CH_3)_3$), 0.88 (m, 6H, $P(CH_2CH_3)_3$), 0.59 (s, 18H, $SiMe_3$), 0.54 (s, 18H, $SiMe_3$), 0.48 (s, 6H, $SiMe_2$), 0.43 (s, 6H, $SiMe_2$). ^{13}C NMR (δ in ppm): 96.3 (Cp), 22.7 ($P(CH_2CH_3)_3$), 9.4 ($P(CH_2CH_3)_3$), 5.6 ($SiMe_3$), 5.4 ($SiMe_3$), 0.3 ($SiMe_2$), 0.1 ($SiMe_2$). ^{29}Si NMR (δ in ppm): −4.1 ($SiMe_3$), −5.0 ($SiMe_3$), −20.1 ($SiMe_2$), −101.4 (quart. Si). ^{31}P NMR (δ in ppm): 50.2 ($^{2}J_{117Sn/119Sn}$ = 232 Hz, 266 Hz). ^{119}Sn NMR(δ in ppm): 1635 (d, $^{1}J_{SnP}$ = 266 Hz). Anal. calcd for $C_{32}H_{73}PSi_8SnTi$ (880.16): C, 43.67; H, 8.36. Found: C, 43.22; H, 8.09.

*Zirconocene Stannylene Phosphine Complex (**6**).* Deep-purple crystals (yield: 85%): ^{1}H NMR (δ in ppm): 5.41 (s, 10H, Cp), 1.05 (m, 9H, $P(CH_2CH_3)_3$), 0.86 (m, 6H, $P(CH_2CH_3)_3$), 0.60 (s, 18H, $SiMe_3$), 0.50 (s, 18H, $SiMe_3$), 0.49 (s, 6H, $SiMe_2$), 0.36 (s, 6H, $SiMe_2$). ^{13}C NMR (δ in ppm): 96.7 (Cp), 20.2 (d, $^{2}J_{PC}$ = 15.8 Hz, $P(CH_2CH_3)_3$), 8.4 ($P(CH_2CH_3)_3$), 5.1 ($SiMe_3$), 4.7 ($SiMe_3$), 3.4 ($SiMe_2$). ^{29}Si NMR (δ in ppm): −5.0 (d, $^{4}J_{PSi}$ = 2.1 Hz, $SiMe_3$), −5.9 (d, $^{4}J_{PSi}$ = 3.2 Hz, $SiMe_3$), −19.4 ($SiMe_2$), −108.2 (d, $^{3}J_{PSi}$ = 1.6 Hz, quart. Si). ^{31}P NMR (δ in ppm): 37.5($^{1}J_{PSn}$ = 133 Hz). ^{119}Sn NMR (δ in ppm): 1263 (d, $^{1}J_{PSn}$ = 133 Hz). Anal. calcd for $C_{32}H_{73}PSi_8SnZr$ (923.51): C, 41.62; H, 7.97. Found: C, 40.96; H, 8.05.

*Hafnocene Stannylene Phosphine Complex (**7**).* Deep-purple crystals (yield: 79%): ^{1}H NMR (δ in ppm): 5.29 (s, 10H, Cp), 1.13 (td, $^{3}J_{HH}$ = 7.6 Hz, $^{3}J_{PH}$ = 13.0 Hz, 9H, $P(CH_2CH_3)_3$), 0.88 (m, 6H, $P(CH_2CH_3)_3$), 0.62 (s, 18H, $SiMe_3$), 0.60 (s, 6H, $SiMe_2$), 0.52 (s, 6H, $SiMe_2$), 0.51 (s, 18H, $SiMe_3$). ^{13}C NMR (δ in ppm): 95.5 (Cp), 22.1 (d, $^{2}J_{PC}$ = 18.9 Hz, $P(CH_2CH_3)_3$), 9.3 ($P(CH_2CH_3)_3$), 5.5 ($SiMe_3$), 5.2 ($SiMe_3$), −0.3 ($SiMe_2$), −0.4 ($SiMe_2$). ^{29}Si NMR (δ in ppm): −4.4 (d, $^{4}J_{PSi}$ = 2.6 Hz, $SiMe_3$), −5.9 (d, $^{4}J_{PSi}$ = 3.6 Hz, $SiMe_3$), −19.0 ($SiMe_2$), −110.8 (d, $^{3}J_{PSi}$ = 3.1 Hz, quart. Si). ^{31}P NMR (δ in ppm): 34.8 (no tin satellites observed). ^{119}Sn NMR (δ in ppm): 1079 (d, $^{2}J_{SnP}$ = 92 Hz). Anal. calcd for $C_{32}H_{73}HfPSi_8Sn$ (1010.78): C, 38.02; H, 7.28. Found: C, 37.73; H, 7.25.

*Titanocene Plumbylene Phosphine Complex (**8**).* Dark-green crystals (yield: 80%): ^{1}H NMR (δ in ppm): 5.2 (s, 10H, Cp), 1.08 (m, 9H, $P(CH_2CH_3)_3$), 0.85 (m, 6H, $P(CH_2CH_3)_3$), 0.62 (s, 18H, $SiMe_3$), 0.58 (s, 18H, $SiMe_3$), 0.52 (s, 6H, $SiMe_2$), 0.37 (s, 6H, $SiMe_2$). ^{13}C NMR (δ in ppm): 96.2 (Cp), 23.0 (d, $^{2}J_{PC}$ = 5.4 Hz, $P(CH_2CH_3)_3$), 6.7 ($SiMe_3$), 6.6 ($SiMe_3$), 4.0 ($SiMe_2$), 3.2 ($SiMe_2$). ^{29}Si NMR (δ in ppm): −2.3 (d, $^{4}J_{PSi}$ = 2.7 Hz, $SiMe_3$), −3.7 (d, $^{4}J_{PSi}$ = 3.8 Hz, $SiMe_3$), −6.9 ($SiMe_2$), −15.6 (d, $^{3}J_{PSi}$ = 2.5 Hz, quart. Si). ^{31}P NMR (δ in ppm): 57.5. ^{207}Pb NMR (δ in ppm): 5299 (fwhm: 217.8 Hz).

*Zirconocene Plumbylene Phosphine Complex (**9**).* Deep-purple crystals (yield: 77%): ^{1}H NMR (δ in ppm): 5.36 (s, 10H, Cp), 1.08 (m, 9H, $P(CH_2CH_3)_3$), 0.85 (m, 6H, $P(CH_2CH_3)_3$), 0.65 (s, 18H, $SiMe_3$), 0.62 (s, 6H, $SiMe_2$), 0.55 (s, 18H, $SiMe_3$), 0.53 (s, 6H, $SiMe_2$). ^{13}C NMR (δ in ppm): 96.5 (Cp), 19.9 (d, $^{2}J_{PC}$ = 15.1 Hz, $P(CH_2CH_3)_3$), 8.6 ($P(CH_2CH_3)_3$), 6.3 ($SiMe_3$), 6.2 ($SiMe_3$), 3.2 ($SiMe_2$),

2.4 ($SiMe_2$). ^{29}Si NMR (δ in ppm): −3.7 (d, $^4J_{PSi}$ = 2.0 Hz, $SiMe_3$), −4.1 (d, $^4J_{PSi}$ = 3.1 Hz, $SiMe_3$), −7.1 ($SiMe_2$), −42.0 (d, $^3J_{PSi}$ = 2.4 Hz, quart. Si). ^{31}P NMR (δ in ppm): 46.3. ^{207}Pb NMR (δ in ppm): 4165 (fwhm: 128.5 Hz).

*Hafnocene Plumbylene Phosphine Complex (**10**).* Deep-purple crystals (yield: 84%): ^1H NMR (δ in ppm): 5.24 (s, 10H, Cp), 1.15 (td, $^3J_{HH}$ = 7.7 Hz, $^3J_{PH}$ = 13.1 Hz, 9H, $P(CH_2CH_3)_3$), 0.87 (m, 6H, $P(CH_2CH_3)_3$), 0.67 (s, 18H, $SiMe_3$), 0.63 (s, 6H, $SiMe_3$), 0.62 (s, 6H, $SiMe_3$), 0.54 (s, 18H, $SiMe_3$). ^{13}C NMR (δ in ppm): 94.6 (Cp), 21.3 (d, $^2J_{PC}$ = 20.2 Hz, $P(CH_2CH_3)_3$), 9.2 ($P(CH_2CH_3)_3$), 6.2 ($SiMe_3$), 6.1 ($SiMe_3$), 2.9 ($SiMe_2$), 2.2 ($SiMe_2$). ^{29}Si NMR (δ in ppm): −2.5 (d, $^4J_{PSi}$ = 2.2 Hz, $SiMe_3$), −4.3 (d, $^4J_{Psi}$ = 3.2 Hz, $SiMe_3$), −7.7 ($SiMe_2$), −53.9 (d, $^3J_{Psi}$ = 3.7 Hz, quart. Si). ^{31}P NMR (δ in ppm): 45.5 (no ^{207}Pb satellites observed). ^{207}Pb NMR (δ in ppm): 3462 (fwhm: 172.1 Hz).

*Hafnocene Bis(Stannylene) Complex (**11**).* A mixture of hafnocene dichloride (20 mg, 0.05 mmol), magnesium turnings (5 mg, 4.8 mmol, excess), and **3** (61 mg, 0.05 mmol) was suspended in THF (5 mL), subjected to ultrasonification, and stirred for 1 h. A black suspension developed. All volatile materials were removed in vacuo, and the residue was extracted with pentane (10 mL). The dark filtrate was concentrated to 3 mL and stored at −60 °C for 60 h. Black needle-shaped crystals of **11** (40 mg, 0.03 mmol, 54%) were isolated upon filtration and dried in vacuo. ^1H NMR (δ in ppm): 4.85 (s, 10H, Cp), 0.47 (s, 36H, $SiMe_3$), 0.46 (s, 36H, $SiMe_3$), 0.29 (s, 12H, $SiMe_2$), 0.25 (s, 12H, $SiMe_2$). ^{13}C NMR (δ in ppm): 96.3 (Cp), 13.9 ($SiMe_2$), 13.8 ($SiMe_2$), 4.9 ($SiMe_3$), 4.8 ($SiMe_3$). ^{29}Si NMR (δ in ppm): −6.8 ($SiMe_3$), −10.8 ($SiMe_3$), −20.1 ($SiMe_2$), −85.3 (quart. Si). ^{119}Sn NMR (δ in ppm): 1785. Anal. calcd for $C_{42}H_{106}HfSi_{16}Sn_2$ (1476.57): C, 34.16; H, 7.24. Found: C, 33.71; H, 7.29.

*Titanocene Bis(stannylene) Complex (**13**).* A mixture of titanocene dichloride (25 mg, 0.10 mmol), magnesium turnings (6 mg, 0.25 mmol), and distannene **3** (117 mg, 0.10 mmol) was suspended in THF (4 mL), subjected to ultrasonification for 2 min, and stirred for 1 h. A deep-purple suspension developed. All volatile materials were removed in vacuo, and the blue residue was extracted 3× with pentane (2 mL each). The dark-blue filtrate was concentrated to 2 mL and stored at −60 °C for 16 h. Blue crystals of **13** (87 mg (0.07 mmol, 70%) were isolated by decantation and dried in vacuo. ^1H NMR (δ in ppm): 5.36 (s, 10H, Cp), 0.46 (s, 72H, $SiMe_3$), 0.34 (s, 24H, $SiMe_2$). ^{13}C NMR (δ in ppm): 94.6 (Cp), 4.7 ($SiMe_3$), −0.4 ($SiMe_2$). ^{29}Si NMR (δ in ppm): −1.7 ($SiMe_3$), −19.4 ($SiMe_2$), −79.0 (quart. Si). ^{119}Sn NMR (δ in ppm): 2172.

The crystals containing $Cp_2TiN(SiMe_3)_2$ were presumably formed by reduction of Cp_2TiCl_2 with magnesium in the presence of a batch of **3** which was contaminated with $KN(SiMe_3)_2$ from the synthesis of **3**. The mixed crystals are green from the Ti(III)-compound but were suitable for X-ray crystallography, whereas from pure **13**, no crystals of good quality could be obtained.

*Hafnocene Bis(Plumbylene) Complex (**15**).* A mixture of hafnocene dichloride (20 mg, 0.05 mmol), magnesium turnings (4 mg, 0.16 mmol), and **4** (67 mg, 0.05 mmol) was suspended in THF (5 mL), subjected to ultrasonification for 2 min, and stirred for 1 h. The suspension developed a red coloration and was evaporated to dryness. Three times extraction with pentane (3 mL each) yielded a black solution which was concentrated to 2 mL and stored at −60 °C for 36 h. Black needle-shaped crystals of **15** (33 mg, 0.02 mmol, 40%) were isolated by decantation and dried in vacuo. All NMR of **15** were measured in pentane with a D_2O capillary. ^1H NMR (δ in ppm): 6.21 (10H, Cp), 0.81 (24H, $SiMe_2$), 0.74 (72H, $SiMe_3$). ^{13}C NMR (δ in ppm): 96.9 (Cp), 6.9 ($SiMe_3$), 3.6($SiMe_2$). ^{29}Si NMR(δ in ppm): 1.0 ($SiMe_3$), −4.9 ($SiMe_2$), −16.6 (quart. Si). ^{207}Pb NMR: no signal was observed.

*Zirconocene Plumbylene Tetrahydrofurane Complex (**16**).* Cp_2ZrCl_2 (100 mg, 0.34 mmol), **4** (114 mg, 0.17 mmol (considered to be monomeric in solution), and magnesium turnings (24 mg, 1.0 mmol, excess) were suspended in THF and subjected to ultrasonification for 5 min. The mixture turned deep red and was stirred for an additional hour. All volatile materials were removed in vacuo, and the black residue was extracted with pentane (3× 3 mL). The red-purple extract was concentrated to 3 mL and stored for 72 h at −60 °C. Purple crystals of **16** (106 mg, 0.11 mmol, 63%) were isolated by decantation and cautiously dried in vacuo. NMR (C_6D_6, rt, δ in ppm): ^1H: 4.82 (s, 10H, Cp), 2.68 (br, 4H, THF), 1.63 (br, 4H, THF), 0.44 (s, 12H, $SiMe_2$), 0.29 (s, 36H, $SiMe_3$). ^{13}C: 95.6 (Cp), 60.6 (THF), 20.1 (THF), 3.5 ($SiMe_3$), 2.0($SiMe_2$). ^{29}Si: −10.0 ($SiMe_3$), −11.3 ($SiMe_2$), −36.7 (quart. Si). ^{207}Pb: 5770.

*Trichlorotantalum Stannylene Diphosphine Complex (**17**).* A mixture of $TaCl_5$ (75 mg, 0.21 mmol), magnesium turnings (12 mg, 0.5 mmol, excess), PEt_3 (50 mg, 0.42 mmol), and **1** (150 mg, 0.21 mmol) were suspended in THF and subjected to ultrasonification for 2 min, during which time the suspension turned purple. The mixture was stirred for 3 h at rt, and then all volatile materials were removed in vacuo. The residue was extracted with pentane (10 mL). The purple extract was concentrated (4 mL) and stored at −60 °C for 48 h. Deep-purple crystals of **17** (107 mg, 0.10 mmol, 46%) were isolated by decantation and dried in vacuo. ^1H NMR (δ in ppm): 2.17 (m, 6H, $P(CH_2CH_3)_3$), 1.05 (m, 9H, $P(CH_2CH_3)_3$), 0.51 (s, 12H, $SiMe_2$), 0.47 (s, 36H, $SiMe_3$). ^{13}C NMR (δ in ppm): 24.2 ($P(CH_2CH_3)_3$), 9.0 ($P(CH_2CH_3)_3$), 4.5 ($SiMe_3$), −0.9 ($SiMe_2$). ^{29}Si NMR (δ in ppm): 6.7 ($SiMe_3$), −18.6 ($SiMe_2$), −105.9 (quart. Si). ^{31}P NMR (δ in ppm): 38.7 (s, $^2J_{PSn}$ = 73 Hz). ^{119}Sn NMR (δ in ppm): 1985 (t, $^2J_{PSn}$ = 73 Hz). Anal. calcd for $C_{28}H_{78}Cl_3P2Si_8SnTa$ (1107.57): C, 30.36; H, 7.10. Found: C, 30.17; H, 7.025.

■ ASSOCIATED CONTENT

Ⓢ Supporting Information

Plots of the molecular structures in the crystal of compounds **5**, **6**, **8**, **9**, **11**, and **15**, tables containing crystallographic data and information for compounds **5**−**10**, and **13** and **14** in CIF format. Details of the calculated structures of compounds **5**−**13**, **15**, **19**−**21** and some additional reference compounds (**22**−**33**). and complete ref 26. This material is available free of charge via the Internet at http://pubs.acs.org.

■ AUTHOR INFORMATION

Corresponding Author

baumgartner@tugraz.at; christoph.marschner@tugraz.at; thomas.mueller@uni-oldenburg.de

Notes

The authors declare no competing financial interest.

■ ACKNOWLEDGMENTS

Support for this study was provided by the Austrian Fonds zur Förderung der wissenschaftlichen Forschung (FWF) via the projects P-19338 (C.M.) and P-21346 (J.B.). P.Z. thanks the Fonds der Chemischen Industrie (FCI) for a scholarship (no.183191). The High-Performance Computing centre at the CvO University is thanked for computer time

■ REFERENCES

(1) Fischer, R. C.; Power, P. P. *Chem. Rev.* **2010**, *110*, 3877−3923.

(2) Ganzer, I.; Hartmann, M.; Frenking, G. In *The Chemistry of Organic Germanium, Tin and Lead Compounds*; Rappoport, Z., Ed.; John Wiley & Sons, Ltd: Chichester, U.K., 2002; Vol. 2, pp 169−282.

(3) Mizuhata, Y.; Sasamori, T.; Tokitoh, N. *Chem. Rev.* **2009**, *109*, 3479−3511.

(4) Lee, V. Y.; Fukawa, T.; Nakamoto, M.; Sekiguchi, A.; Tumanskii, B. L.; Karni, M.; Apeloig, Y. *J. Am. Chem. Soc.* **2006**, *128*, 11643−11651.

(5) Klinkhammer, K. W.; Schwarz, W. *Angew. Chem., Int. Ed. Engl.* **1995**, *34*, 1334−1336.

(6) Arp, H.; Baumgartner, J.; Marschner, C.; Müller, T. *J. Am. Chem. Soc.* **2011**, *133*, 5632−5635.

(7) Arp, H.; Baumgartner, J.; Marschner, C.; Zark, P.; Müller, T *J. Am. Chem. Soc.* **2012**, *134*, 6409−6415.

(8) Whittal, R. M.; Ferguson, G.; Gallagher, J. F.; Piers, W. E. *J. Am. Chem. Soc.* **1991**, *113*, 9867−9868.

(9) Piers, W. E.; Whittal, R. M.; Ferguson, G.; Gallagher, J. F.; Froese, R. D. J.; Stronks, H. J.; Krygsman, P. H. *Organometallics* **1992**, *11*, 4015−4022.
(10) Davidson, P. J.; Harris, D. H.; Lappert, M. F. *J. Chem. Soc., Dalton Trans.* **1976**, 2268−2274.
(11) Bares, J.; Richard, P.; Meunier, P.; Pirio, N.; Padelkova, Z.; Cernosek, Z.; Cisarova, I.; Ruzicka, A. *Organometallics* **2009**, *28*, 3105−3108.
(12) Nakata, N.; Fujita, T.; Sekiguchi, A. *J. Am. Chem. Soc.* **2006**, *128*, 16024−16025.
(13) Heitmann, D.; Pape, T.; Hepp, A.; Mück-Lichtenfeld, C.; Grimme, S.; Hahn, F. E. *J. Am. Chem. Soc.* **2011**, *133*, 11118−11120.
(14) Negishi, E.; Takahashi, T. *Bull. Chem. Soc. Jpn.* **1998**, *71*, 755−769.
(15) Burlakov, V. V.; Polyakov, A. V.; Yanovsky, A. I.; Struchkov, Y. T.; Shur, V. B.; Vol'pin, M. E.; Rosenthal, U.; Görls, H. *J. Organomet. Chem.* **1994**, *476*, 197−206.
(16) Rosenthal, U.; Ohff, A.; Michalik, M.; Görls, H.; Burlakov, V. V.; Shur, V. B. *Angew. Chem.* **1993**, *105*, 1228−1230.
(17) Sharma, H. K.; Haiduc, I.; Pannell, K. H. In *The Chemistry of Organic Germanium, Tin and Lead Compounds*; Rappoport, Z., Ed.; John Wiley & Sons, Ltd: Chichester, U.K., 2002; Vol. *2* , pp 1241−1332.
(18) Zirngast, M.; Flock, M.; Baumgartner, J.; Marschner, C. *J. Am. Chem. Soc.* **2009**, *131*, 15952−15962.
(19) Masamune, S.; Sita, L. R. *J. Am. Chem. Soc.* **1985**, *107*, 6390−6391.
(20) Katir, N.; Matioszek, D.; Ladeira, S.; Escudié, J.; Castel, A. *Angew. Chem., Int. Ed.* **2011**, *50*, 5352−5355.
(21) Herberhold, M.; Tröbs, V.; Milius, W.; Wrackmeyer, B. *Z. Naturforsch., B* **1994**, *49*, 1781−1788.
(22) Cordero, B.; Gomez, V.; Platero-Prats, A. E.; Reves, M.; Echeverria, J.; Cremades, E.; Barragan, F.; Alvarez, S. *Dalton Trans.* **2008**, 2832−2838.
(23) Pyykkö, P.; Atsumi, M. *Chem.—Eur. J.* **2009**, *15*, 12770−12779.
(24) Lukens, W. W.; Smith, M. R.; Andersen, R. A. *J. Am. Chem. Soc.* **1996**, *118*, 1719−1728.
(25) Feldman, J.; Calabrese, J. C. *J. Chem. Soc., Chem. Commun.* **1991**, 1042−1044.
(26) Frisch, M. J.; Trucks, G. W.;et al. *Gaussian 09*, revision B.01; Gaussian, Inc.: Wallingford, CT, 2010. For detailed description of the computations, see the Supporting Information.
(27) Details of these computed structures are discussed elsewhere; see ref 6, 7.
(28) The dihedral angle β is defined by the EMP- and the SiESi planes in the monotetrylene complexes and by the EME and SiESi planes in the bis(tetrylene) complexes.
(29) Müller, T. *J. Organomet. Chem.* **2003**, *686*, 251−256 and refs given there.
(30) For the lead compounds, the following orbital energies were obtained: $E(\sigma)$ = −6.04 eV (**8**), −6.11 eV (**9**), −6.11 eV (**10**), $E(\pi^*)$ = −1.00 eV (**8**), −0.71 eV (**9**), −0.56 eV (**10**).
(31) Mantina, M.; Chamberlin, A. C.; Valero, R.; Cramer, C. J.; Truhlar, D. G. *J. Phys. Chem. A* **2009**, *113*, 5806−5812.
(32) Zhao, Y.; Truhlar, D. G. *Theor. Chem. Acc.* **2007**, *120*, 215−241.
(33) Sieffert, N.; Bühl, M. *Inorg. Chem.* **2009**, *48*, 4622−4624.
(34) Schreiner, P. R.; Chernish, L. V.; Gunchenko, P. A.; Tikhonchuk, E. Y.; Hausmann, H.; Serafin, M.; Schlecht, S.; Dahl, J. E. P.; Carlson, R. M. K.; Fokin, A. A. *Nature* **2011**, *477*, 308−311.
(35) Grimme, S.; Schreiner, P. R. *Angew. Chem., Int. Ed.* **2011**, *50*, 12639−12642.
(36) Pangborn, A. B.; Giardello, M. A.; Grubbs, R. H.; Rosen, R. K.; Timmers, F. J. *Organometallics* **1996**, *15*, 1518−1520.
(37) Helmer, B. J.; West, R. *Organometallics* **1982**, *1*, 877−879.
(38) Morris, G. A.; Freeman, R. *J. Am. Chem. Soc.* **1979**, *101*, 760−762.
(39) *SAINTPLUS: Software Reference Manual*, version 6.45; Bruker-AXS: Madison, WI, 1997−2003.
(40) Blessing, R. H. *Acta Crystallogr., Sect. A* **1995**, *51*, 33−38.
(41) *SADABS*, version 2.1 Bruker-AXS: Madison, WI, 1998.
(42) Sheldrick, G. M. *Acta Crystallogr., Sect. A* **2008**, *64*, 112−122.